Intrinsic Optical Absorption in Germanium-Silicon Alloys

RUBIN BRAUNSTEIN, ARNOLD R. MOORE, AND FRANK HERMAN
RCA Laboratories, Princeton, New Jersey
(Received October 4, 1957)

The intrinsic optical absorption spectrum for the germanium-silicon alloy system has been measured as a function of temperature and composition. Over the entire composition range the absorption near the threshold ($K<100$ cm^{-1}) exhibits a temperature dependence which is characteristic of phonon-assisted indirect electronic transitions. There appears to be no temperature-independent component of the absorption attributable to disorder-assisted transitions. When the phonon contribution to the absorption is explicitly taken into account, as in a Macfarlane-Roberts type analysis, the experimental data yield an equivalent phonon temperature which varies from 270±20°K for pure Ge to 550±50°K for pure Si, with most of the variation occurring in the middle of the composition range. The composition dependence of the derived energy gap shows an abrupt change in slope at about 15 atomic percent Si. This is due to a switch from a Ge-like ([111]) to a Si-like ([100]) conduction band structure. The onset of direct electronic transitions (10^2 cm$^{-1}<K<10^4$ cm^{-1}) was observed as a function of composition in the Ge-rich alloys. The data show that the [000] conduction band minimum moves more rapidly than the [111] minima as Si is added to Ge. In an attempt to account for the observed variation of the phonon equivalent temperature with composition, certain lattice vibrational modes were computed on the basis of a number of simplified models. The one which gives the most realistic results emphasizes the presence of atoms of different masses and some short-range order in the alloy lattice.

1. INTRODUCTION

THE intrinsic optical properties of nearly perfect semiconducting crystals have been extensively investigated, and a great deal of experimental information is now available for a wide variety of such crystals.[1] By examining the absorption spectrum and its temperature dependence in terms of existing theories, it is often possible to obtain important information bearing on the energy band structure, as well as a clue to the nature of the mechanisms responsible for the absorption in the neighborhood of the threshold.

For example, in silicon and germanium, optical studies[1–4] confirm the fact that the valence and conduction band edges are located at different positions in the reduced zone. They also indicate that indirect electronic transitions assisted by phonons are responsible for most of the absorption near the threshold. (These transitions involve the creation of electron-hole pairs; in order to conserve crystal momentum, phonons of appropriate wave number are created or destroyed.) Recent high-resolution work[5,6] on these two materials suggests that exciton formation,[7,8] accompanied by the creation or destruction of momentum-conserving phonons, is responsible for some of the absorption near the threshold.

Although a considerable amount of experimental work has also been done on the optical properties of nondilute semiconducting alloys,[9] the absorption mechanisms operating in such materials are obscure. Most workers in this field have been content to study the variation of the absorption threshold with composition, usually at a fixed temperature, since this provides a rough picture of the composition dependence of the energy gap. To our knowledge, no systematic attempt has yet been made to interpret the experimental data in such a manner as to shed some light on the role that disorder plays in relaxing the optical selection rules which obtain in ordered crystals.[10]

The present investigation of the germanium-silicon alloy system was undertaken with two objectives in mind. In the first place, we wanted to study the absorption spectrum as a function of composition in somewhat greater detail than had been done previously,[11] in order to obtain more precise information about the band structure of the alloy system. Secondly, we wanted to obtain experimental information which could be analyzed so as to permit a distinction to be made between phonon-assisted and disorder-assisted absorption near the threshold.

The decision to study the germanium-silicon alloy system in preference to other alloy systems was based on the following considerations. Germanium and silicon are miscible in all proportions, forming a continuous series of solid substitutional solutions of fixed crystal structure over the entire composition range. Since fairly homogeneous single crystal or polycrystalline specimens of high purity and of arbitrary composition can be prepared, it is possible to study the optical properties as a function of composition over the entire range of compositions. Furthermore, the energy band structure

[1] H. Y. Fan, Repts. Progr. Phys. **19**, 107 (1956); Burstein, Pucus, and Sclar, *Proceedings of the Conference on Photoconductivity, Atlantic City, November, 1954* (John Wiley and Sons, Inc., New York, 1956), p. 353. Bardeen, Blatt, and Hall, *ibid.*, p. 146; Fan, Shepherd, and Spitzer, *ibid.*, p. 184.
[2] G. G. Macfarlane and V. Roberts, Phys. Rev. **97**, 1714 (1955).
[3] G. G. Macfarlane and V. Roberts, Phys. Rev. **98**, 1865 (1955).
[4] W. C. Dash and R. Newman, Phys. Rev. **99**, 1151 (1955).
[5] Macfarlane, McLean, Quarrington, and Roberts, Phys. Rev. **108**, 1377 (1957).
[6] R. A. Smith (private communication).
[7] G. Dresselhaus, J. Phys. Chem. Solids **1**, 15 (1956).
[8] R. J. Elliott, Phys. Rev. **108**, 1384 (1957).
[9] For a discussion and an extensive list of references, see Herman, Glicksman, and Parmenter, *Progress in Semiconductors* (Heywood and Company, Ltd., London, 1957), Vol. 2, p. 1.
[10] D. L. Dexter, *Proceedings of the Conference on Photoconductivity, Atlantic City, November, 1954* (John Wiley and Sons, Inc., New York, 1956), p. 155.
[11] E. R. Johnson and S. M. Christian, Phys. Rev. **95**, 560 (1954).

and the optical properties of the pure constituents are fairly well understood,[1–8,12] and this considerably simplifies the task of interpreting the data for the intermediate alloys.

In brief, the absorption spectrum near the threshold was determined both as a function of composition and temperature. The absorption exhibited a marked temperature dependence, of the same type as is observed in pure germanium and pure silicon, over the entire composition range. This leads us to the conclusion that the primary absorption mechanism near the threshold is the same for Ge-Si alloys as for pure Ge and Si, namely, phonon-assisted indirect electronic transitions. Our measurements failed to reveal any temperature-independent component of the absorption which could be attributed to disorder-assisted electronic transitions.

The absorption data at low absorption levels was fitted to the Macfarlane-Roberts expression[2,3]:

$$K(h\nu,T)=A\left[\frac{(h\nu-E_g-k\theta)^2}{1-\exp(-\theta/T)}+\frac{(h\nu-E_g+k\theta)^2}{\exp(\theta/T)-1}\right], \quad (1)$$

where K is the absorption coefficient (in cm^{-1}), $h\nu$ the photon energy, $k\theta$ the phonon energy, E_g the energy gap, T the absolute temperature, and A a substantially temperature-independent proportionality factor. In the first term, $h\nu \geq E_g+k\theta$, while in the second, $h\nu \leq E_g-k\theta$. This expression describes the absorption due to indirect electronic transitions involving the creation and the destruction of phonons of a given energy ($k\theta$).

If the phonons most effective in assisting the indirect transitions actually belong to a single branch of the vibrational spectrum, the above expression suffices to give their energy correctly. If the effective phonons belong to more than one branch, as is undoubtedly the case in pure Ge and Si and in the Ge-Si alloy system, an analysis based on this expression yields an average phonon energy which may be taken as a characteristic of any particular sample. In practice, it was found that the absorption spectrum for each sample studied could be fitted quite nicely by (1).

Our analysis of the absorption data at low absorption levels on the basis of (1) leads to information concerning (*a*) the composition dependence of E_g, the energy separation between the top of the valence band and the bottom of the conduction band; (*b*) the composition dependence of dE_g/dT; and (*c*), the composition dependence of $k\theta$, the average phonon energy.

The results for (*a*) agree qualitatively with those first reported by Johnson and Christian,[11] in that an abrupt change in the slope of the E_g *vs* composition curve occurs at about 15 atomic percent Si. This abrupt change has been interpreted[12,13] as a switch-over of the conduction band edge from the [111] minima characteristic of pure Ge and Ge-rich alloys to the [100] minima characteristic of pure Si and Si-rich alloys. The correctness of this interpretation has since been confirmed by magnetoresistance measurements.[14,15] The quantity dE_g/dT is found to vary quadratically with T at low temperatures, and linearly with T at moderate temperatures at all compositions. The results for (*b*) indicate a more rapid variation of dE_g/dT with composition for germanium-like band structures than for silicon-like band structures.

As for (*c*), the picture of the variation of the average phonon energy with composition is that $k\theta$ is nearly independent of composition at both ends of the range, and undergoes a fairly rapid change near the center. The composition dependence of the energy of certain short wavelength modes has been computed on the basis of a model consisting of two series of ordered Ge-Si crystals. Four possible types of behavior are revealed. One of these, arising from the crystal series with somewhat more short-range order, resembles the observed behavior.

We have also been able to follow the variation with composition of the threshold for direct transitions in the Ge-rich alloys. By comparing this with that for indirect transitions, it was found that the [000] conduction band minimum moves away from the valence band edge at approximately twice the rate of the [111] minima, as silicon is added to germanium.

2. EXPERIMENTAL SAMPLES AND APPARATUS

The pure germanium and silicon samples were cut from high-resistivity (Ge>30 ohm-cm, Si>50 ohm-cm) single crystals grown by the usual vertical pulling method. The method of preparation of the alloy samples depended on composition range. Low and intermediate Si content samples were grown in a horizontal boat with suitable adjustment of the initial charge concentration to yield the required composition; high Si content crystals were grown by vertical pulling.[16] The samples were single crystals in the range of 0 to 20% Si in Ge and again single from 90 to 100% Si in Ge. Intermediate compositions were coarse polycrystals. The compositions were determined by spectrographic techniques.[17] The silicon content was determined in samples with 0–70 mole percent silicon, while the germanium content was determined in the 70–100 mole percent silicon samples; the silicon or germanium content in these respective ranges was determined to ±5% of the amount present. Most alloy samples were above 5 ohm-cm resistivity. However, the constancy of the room temperature transmission over the long-wavelength region beyond the absorption edge was taken as a criterion of adequate purity, rather than the

[12] F. Herman, Proc. Inst. Radio Engrs. **43**, 1703 (1955).
[13] F. Herman, Phys. Rev. **95**, 847 (1954).
[14] M. Glicksman, Phys. Rev. **100**, 1146 (1955); **102**, 1496 (1956).
[15] M. Glickman and S. M. Christian, Phys. Rev. **104**, 1278 (1956).
[16] S. M. Christian (to be published).
[17] M. C. Gardels and H. H. Whitaker, Anal. Chem. (to be published).

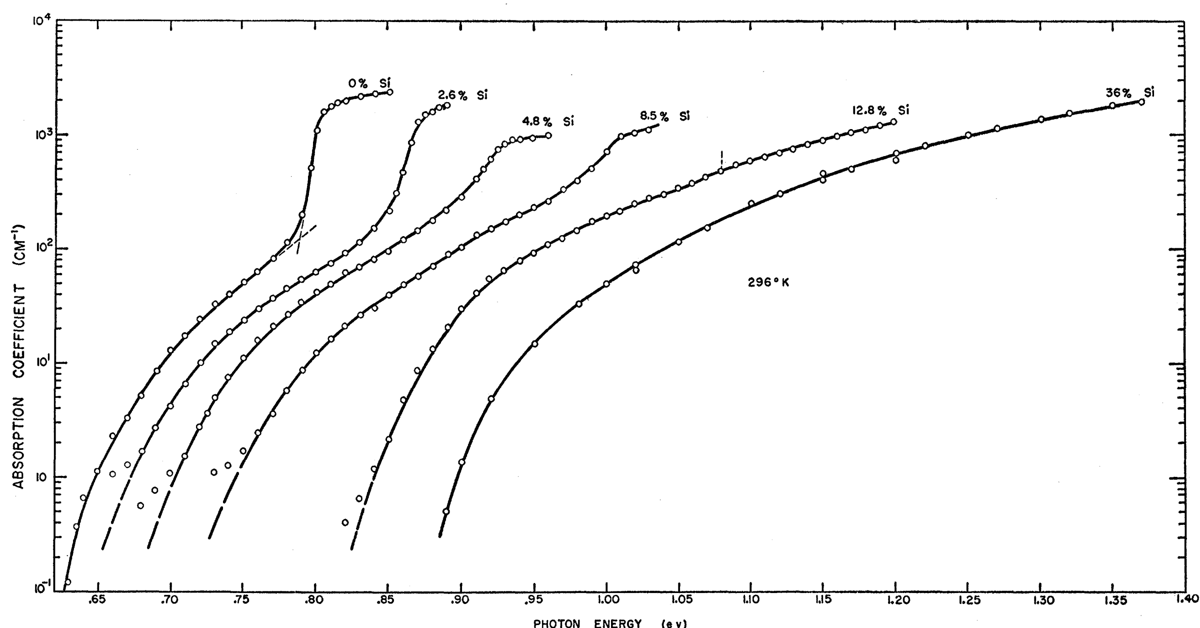

FIG. 1. Intrinsic absorption spectra in a series of Ge-rich Ge-Si alloys at 296°K.

resistivity. Thus the effect of free-carrier absorption was minimized as much as possible in all samples selected for measurement. In the range of composition where both single crystal and polycrystalline samples were available, measurements of the absorption edges yielded identical results, justifying the use of polycrystalline samples.

For measurements in the range of absorption coefficient $(K)<100\ \mathrm{cm}^{-1}$ samples were about 0.5 mm thick, ground and polished on both sides to an optical surface of satisfactory flatness. Transmission measurements after successive repolishing gave identical results, showing that a constant reproducible reflectivity had been obtained. In order to measure $K>100\ \mathrm{cm}^{-1}$ thinner samples were required. For accurate results at $K\sim10^4\ \mathrm{cm}^{-1}$ or greater the samples had to be as thin as $5\ \mu$. These were prepared by mounting thicker pieces on a glass or sapphire slide with glycol phthalate resin and polishing to size, as described by Dash and Newman.[4] Some alloy samples contained grain boundaries and mechanically weak sections, so care had to be taken to avoid breakage or pinholes. In cases where inferior regions developed, the samples were masked to avoid them.

The thickness of the thicker samples was measured with a micrometer or dial gauge to 0.1-mil accuracy. The most convenient method of measurement for thin samples was by analysis of the interference spectrum using the value of the index of refraction calculated from the transmission at long wavelengths for the composition in question. Because of unavoidable fluctuations in composition between slices from the same ingot, a given complete K *versus* photon energy curve was always taken on the same sample progressively thinned down from 500 to 5 microns.

For measurements between room temperatures and liquid nitrogen temperature, the sample was mounted in a stainless steel evacuated Dewar on an apertured copper block in contact with the cooling bath. Fixed temperatures were obtained with constant temperature mixtures such as freon, dry ice-acetone, and liquid nitrogen. A thermocouple mounted on the copper block adjacent to the sample showed less than one degree temperature drop between cooling bath and sample mount. Similar results were obtained with the thermocouple attached directly to the sample. Various types of cements were used to insure good thermal contact of the sample to the copper. This is important for thin samples in which the lateral heat conduction is low. G.E. 7031 calorimeter cement[18] and a cement composed of silver paste in Duco cement were found satisfactory.

Temperatures below 78°K were reached by the use of liquid helium in a double Dewar with quartz windows of the type described by Johnson and Studer.[19] A thermocouple and a carbon resistance thermometer (Allen-Bradley 0.1-watt 40-ohm resistor) were mounted on the copper crystal holder. Attachment of the crystal to the copper block was as described above.

The optical system consisted of a Perkin-Elmer prism monochromator with a tungsten lamp as the light source, a series of spherical and plane mirrors to focus the exit beam onto the sample of the Dewar, and and finally additional mirrors to focus the transmitted beam onto the detector. Special care was taken to

[18] Kindly supplied by Dr. R. Newman of General Electric Research Laboratory.

[19] P. Johnson and F. Studer, Phys. Rev. 82, 976 (1951).

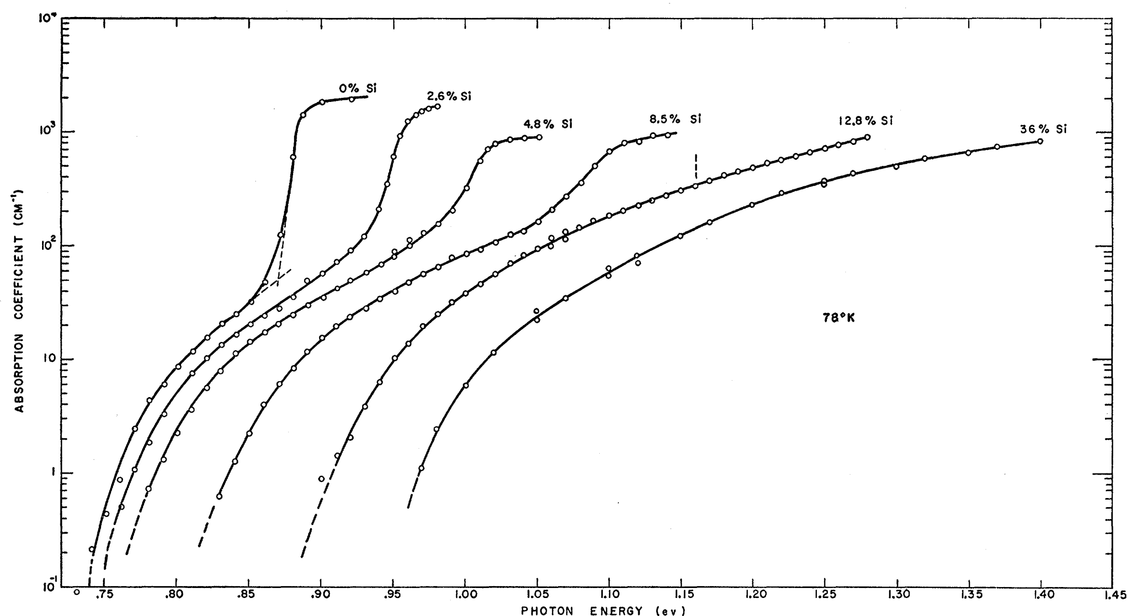

FIG. 2. Intrinsic absorption spectra in a series of Ge-rich Ge-Si alloys at 78°K.

insure that all the light transmitted by the sample was focussed on the detector, even allowing for some scattering at the surface of the sample. Either a dense flint glass or a fused quartz prism was used to get maximum dispersion in the various parts of the spectrum. Over that part of the spectrum corresponding to $K<100$ cm^{-1} the slit width was adjusted to yield an optical band width of about 0.002 ev. Other data were taken with band widths of 0.002 to 0.005 ev. The light was chopped at the source and measured by a phase-sensitive ac amplifier and either a PbS cell or a photomultiplier (RCA 931), depending on the spectral region. A thermocouple was used as a standard.

Correction for reflectance of the sample was accomplished by moving the entire Dewar so that the sample was in or out of the beam. The correction equation given by Fan and Becker[20] was used where applicable. Corrections for the effect of sample backing on thin sections were not necessary since comparison of backed and unbacked samples showed the results to be identical.

3. EXPERIMENTAL RESULTS

The absorption spectra of pure Ge, pure Si, and a number of Ge-Si alloys were determined at 78°K, 196°K, 235°K, and at room temperature. The variation of the absorption spectrum as a function of composition at 296°K and 78°K is depicted in Figs. 1 and 2 for some Ge-rich samples, and in Figs. 3 and 4 for some Si-rich samples. As Si is added to Ge, the absorption curve shifts to higher energy, as was already shown in the preliminary work of Johnson and Christian.[12] Figures 1 and 2 also show a gradual change in the character of the curve at high absorption levels: as the Si content increases, the second rise in K gradually diminishes, until at about 13% Si it is almost absent. Beyond this composition, the curves are very similar in appearance

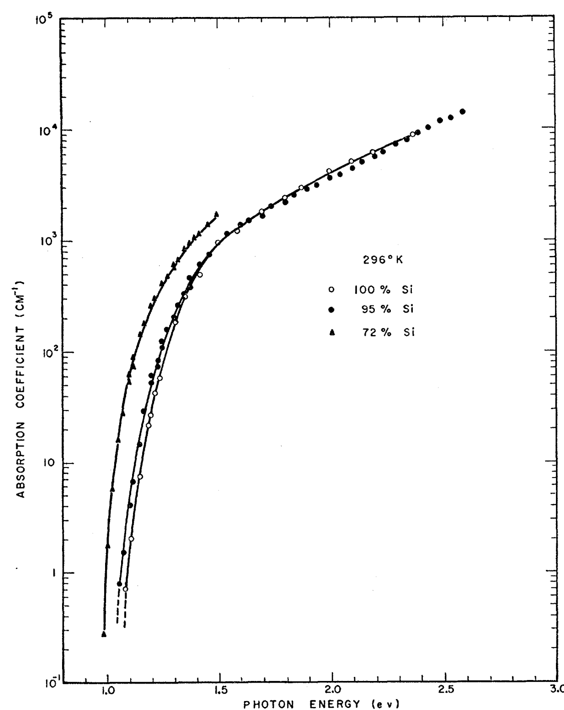

FIG. 3. Intrinsic absorption spectra in a series of Si-rich Ge-Si alloys at 296°K.

[20] H. Y. Fan and M. Becker, *Semiconducting Materials* (Butterworths Scientific Publications, London, 1951), p. 132.

to that of pure Si, except for a displacement on the energy scale.

At the other end of the composition range, the absorption curve shifts to lower energy as Ge is added to Si. There is very little change in shape, except that even a small addition of Ge removes the already slight second rise at 78°K. The first rise in the absorption coefficient is due to indirect electronic transitions, while the second is due to direct electronic transitions.[2–4] According to theory,[1] the absorption coefficient for the latter should exhibit a power law dependence on photon energy. However, if we subtract off that part of the absorption which is due to indirect transitions, the residue cannot be so represented, as has already been pointed out by Dash and Newman.[4] For pure Ge, the residue follows an exponential, rather than a power law.

Note added in proof.—This discrepancy might be resolved when the absorption due to vertical transitions is decomposed into a purely electronic component (direct vertical transitions) and an optical phonon-assisted component (indirect vertical transitions).*

Since a satisfactory theory for the direct transition is not available, the extrapolated intersection of the slowly rising and rapidly rising regions was arbitrarily selected as a measure of the threshold for direct transitions. The variation of this threshold with composition

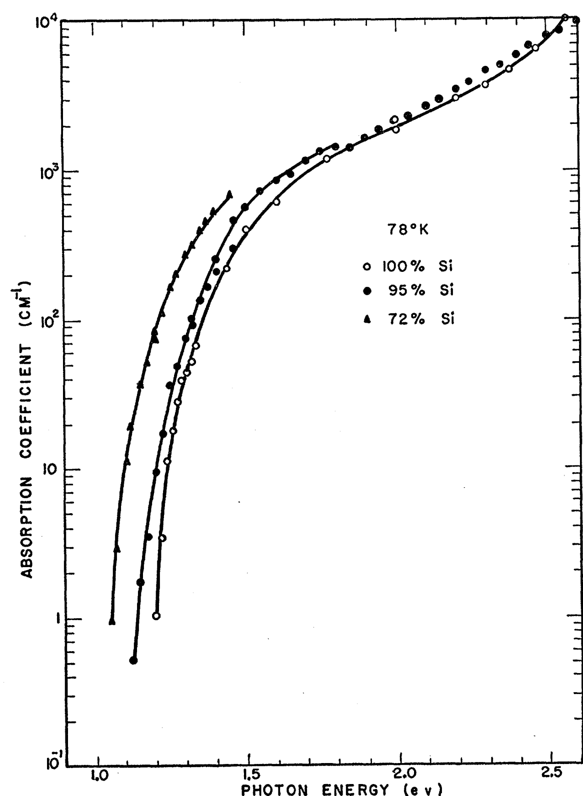

FIG. 4. Intrinsic absorption spectra in a series of Si-rich Ge-Si alloys at 78°K.

* Cf. W. P. Dumke, Phys. Rev. **108**, 1419 (1958).

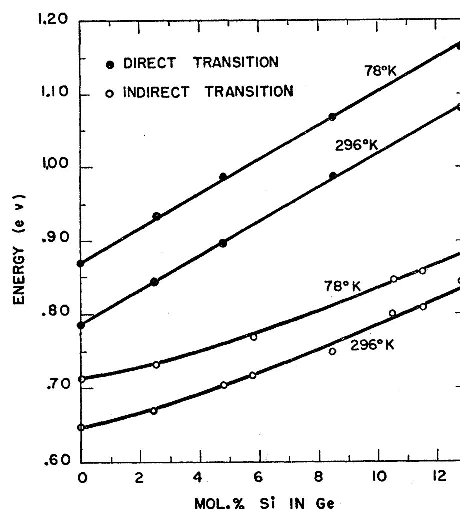

FIG. 5. Energy separation between initial and final electronic states for direct and indirect optical transitions. The energy separation for direct transitions measures the width of the forbidden band at $\mathbf{k}=[000]$. The energy separation for indirect transitions, which measures the energy gap, was taken from Fig. 17 below.

at 78°K and 296°K is shown in Fig. 5. For purposes of comparison, the indirect transition threshold, as determined by methods described below, is also plotted in Fig. 5. It should be noted that the rate at which the direct transition moves with added silicon is a little less than twice the rate of the indirect transition. The "intersection" criterion yields a result of 0.79 ev for the direct transition threshold in pure Ge at room temperature. The corresponding value obtained by Zwerdling and Lax[21] from the oscillatory magnetoabsorption effect is 0.803±0.001 ev.

At the other end of the composition range, the situation is more obscure. Pure Si shows no clearly defined second rise at room temperature, and only a poorly defined one at 78°K. The addition of Ge does nothing to clarify this result.

A detailed study of the low absorption coefficient region ($K<100$ cm^{-1}) was made on pure Ge and Si and another series of alloys as a function of temperature. For the pure Ge and Si samples measurements were taken from room temperature to 5°K. The results are shown in Figs. 6 and 7, respectively. The curves can be decomposed into approximately two linear sections when plotted as $\sqrt{K}$ *versus* photon energy. Aside from the shift to higher energy and changes in slope in going from germanium to silicon, the slopes of the curves are similar. The more obvious difference is the change in the temperature dependence of the slopes. The data so represented are in good agreement with those of Macfarlane and Roberts.[2,3] This breakup into straight-line sections is not as apparent in the results of Dash and Newman[4] or Fan *et al.*[1]

[21] S. Zwerdling and B. Lax, Phys. Rev. **106**, 51 (1957).

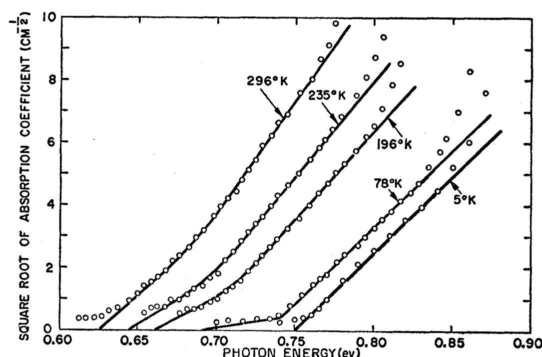

FIG. 6. Dependence of absorption coefficient on photon energy for pure Ge at various temperatures.

Nineteen different alloy compositions were studied covering the complete composition range. Typical results in this series are shown in Figs. 8–11, where the data are plotted as $\sqrt{K}$ *versus* $h\nu$ and again show approximately two straight-line segments, as do the pure components.

The solid lines in Figs. 6 through 11 represent calculated curves that were obtained by fitting appropriate values of θ and E_g to Eq. (1). The curves were fitted for each composition by finding a value of θ which best represented the data at all temperatures, and then determining E_g at each temperature. In view of the approximate nature of the representation afforded by Eq. (1), the agreement between the experimental data and the calculated curves is remarkable.

The values of θ thus determined are plotted as a function of composition in Fig. 12. While the curve-fitting procedure yields fairly well defined values of θ, there is a range of uncertainty for each result. It should be clearly understood that the indicated uncertainty in θ (see vertical lines in Fig. 12) is not an experimental one, but rather an uncertainty arising from the curve-fitting procedure. The uncertainty is smaller for low values of θ because the slopes in the corresponding set of curves are more sensitive to temperature. The significance of the information contained in this figure will be considered in the next section.

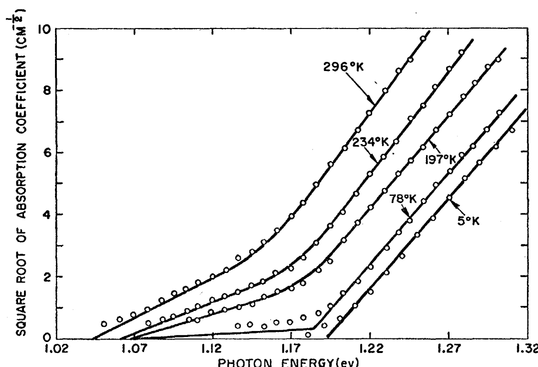

FIG. 7. Dependence of absorption coefficient on photon energy for pure Si at various temperatures.

The variation of E_g with temperature and composition is shown in Figs. 13 and 14. For pure Ge and Si, the data extended to liquid helium temperature exhibit the quadratic temperature dependence first pointed out by Macfarlane and Roberts.[2–3] Our results agree with theirs within a few percent. While a fully satisfactory theory of the temperature dependence of the energy gap in a semiconductor has not yet been worked out, existing theories[22] agree in predicting a quadratic temperature dependence at low temperatures, and a linear temperature dependence at higher temperatures.

Our work indicates that the general shape of the E *vs* T curve remains the same throughout the entire

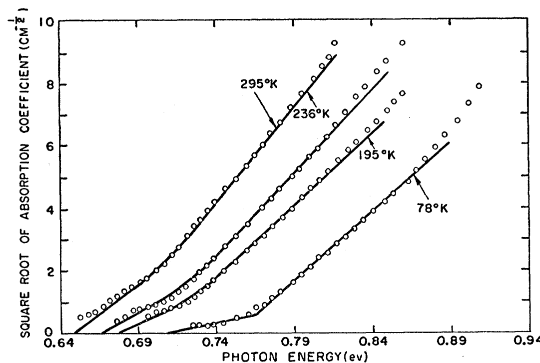

FIG. 8. Dependence of absorption coefficient on photon energy at various temperatures for a Ge-Si alloy with 2.5% Si.

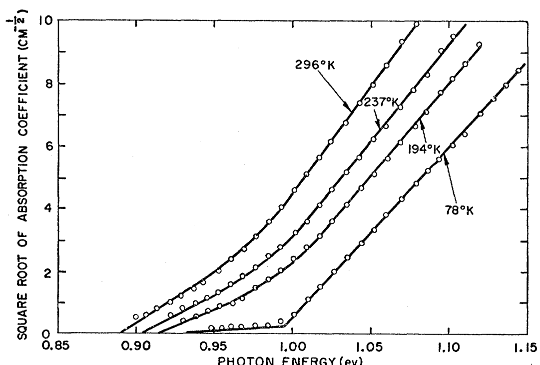

FIG. 9. Dependence of absorption coefficient on photon energy at various temperatures for a Ge-Si alloy with 42.0% Si.

composition range, although the explicit variation of E_g with T changes systematically with composition. In particular, $E_g(296°\text{K})-E_g(78°\text{K})$ decreases rapidly as Si is added to Ge, goes through a minimum in the middle of the composition range, and then increases slowly as pure Si is approached (Fig. 15).

That the temperature coefficient is found to be a more sensitive function of composition in the 0–15% Si range than in the 15–100% Si range is consistent with

[22] E. N. Adams, Phys. Rev. **107**, 671, 698 (1957); H. D. Vasileff, Phys. Rev. **105**, 441 (1957); E. Antoncik, Czechoslov. J. Phys. **5**, 4 (1955).

the fact that the conduction band structure is defined by different sets of minima in these two ranges, i.e., by [111] minima in the former range, and by [100] minima in the latter.

The variation of the photon energy for the half-transmission point with composition at room temperature is displayed in Fig. 16. A sample thickness of 0.020 in. is assumed. A similar curve is obtained if the one-third transmission points are used. The present work confirms the discontinuity in slope of the E_g *vs* composition curve at about 15 mole percent Si first reported by Johnson and Christian.[12] While their curve consisted of two essentially linear portions having different slopes, our curve is nearly linear in the 0–15 mole percent Si range, and quadratic, with positive curvature, in the remainder of the composition range.

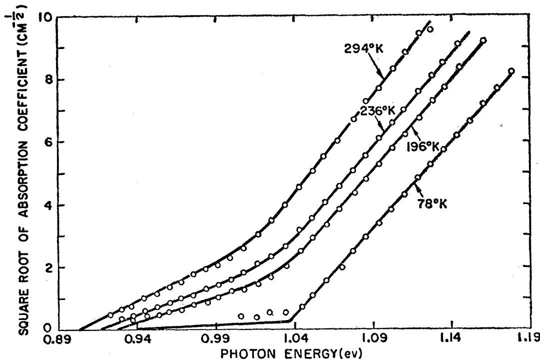

FIG. 10. Dependence of absorption coefficient on photon energy at various temperatures for a Ge-Si alloy with 68.0% Si.

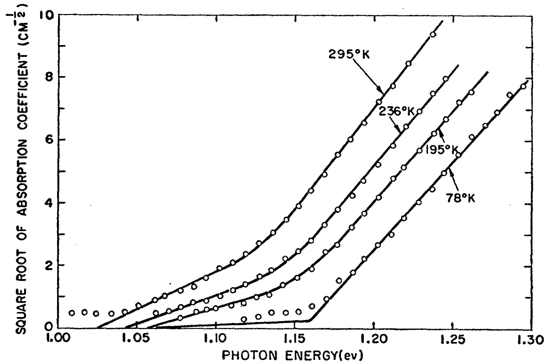

FIG. 11. Dependence of absorption coefficient on photon energy at various temperatures for a Ge-Si alloy with 95.7% Si.

The discrepancy between the earlier data[12] and our own appears to be due largely to the higher purity of our samples. In addition, the compositions of our samples were determined with somewhat greater precision than in the earlier work. In the Johnson and Christian work, an arbitrary point on the transmission curve was taken as a measure of the band gap, just as was done in arriving at Fig. 16. This procedure can lead to systematic errors, especially if the samples used have high free-carrier absorptions.

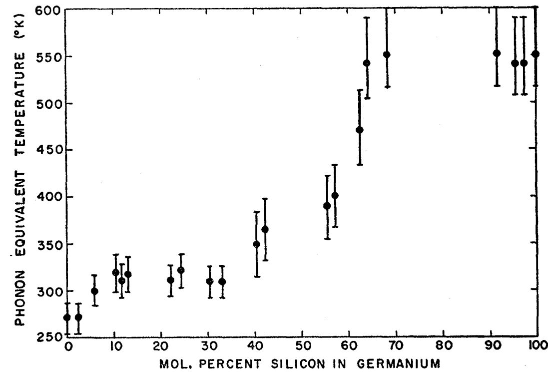

FIG. 12. Composition dependence of equivalent temperature of phonons participating in indirect electronic transitions in Ge-Si alloys. Based on one-phonon Macfarland-Roberts expression; see Eq. (1) in text.

While Fig. 16 gives a rough picture of the E_g *vs* composition curve, it is not correct to the extent that the absorption and emission of phonons are not taken into account. The E_g *vs* composition curve, corrected for phonon absorption and emission, is shown in Fig. 17. The values of E_g appearing in this figure were obtained by fitting the absorption spectra to Eq. (1), as has already been described above.

While the curves in Figs. 16 and 17 are similar in form, they differ in detail since the phonon energy varies with composition.

If the upper portion of the curve in Fig. 17 is extrapolated to pure Ge (see dotted line) it is found that the

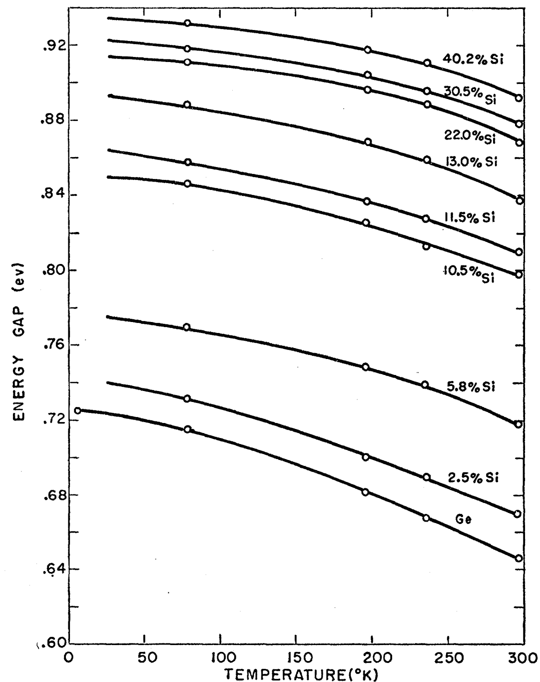

FIG. 13. Temperature dependence of energy gap for a series of Ge-rich Ge-Si alloys.

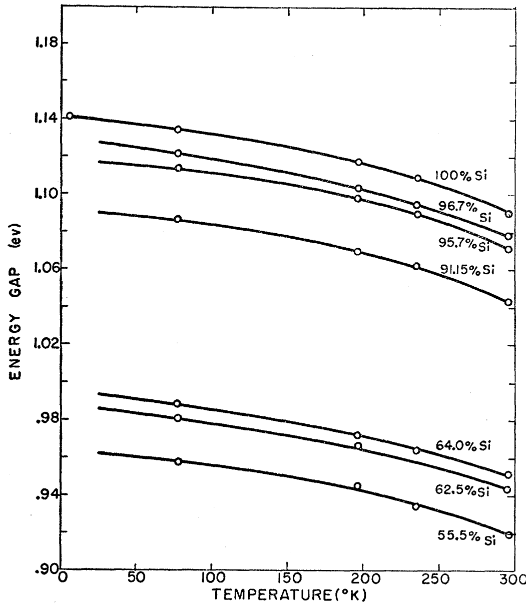

FIG. 14. Temperature dependence of energy gap for a series of Si-rich Ge-Si alloys.

[100] conduction band minima in pure Ge lie approximately 0.22 ev above the [111] minima. Returning to Fig. 5 for a moment, we see that at room temperature the [000] conduction band minimum lies about 0.14 ev above the [111] minima. In the Ge-rich composition range, the [000] minima are found to move away from the valence band edge almost twice as fast as the [111] minima as Si is added to Ge. Since the [000] minimum moves upward on the energy scale much more rapidly than the [111] and the [100] minima, the conduction band edge is never defined by the [000] minimum. Instead, the conduction band edge is defined by the [111] minima in the 0–15 percent Si range, and by the [100] minima in the remainder of the composition range.

4. DISCUSSION

Thus far, it has been assumed that significant information can be obtained by fitting the experimental data to the one-phonon Macfarlane-Roberts expression [see Eq. (1) above]. The use of this expression to represent the absorption data requires some justification on two counts:

First, indirect electronic transitions in an ordered crystal (pure Ge or Si) can be assisted by phonons belonging to different branches of the vibrational spectrum. While these several phonons will have a common reduced wave vector, they may have widely different energies. Therefore, the value of $k\theta$ obtained from Eq. (1) must represent a suitably averaged phonon energy, rather than the energy of a phonon belonging to a particular branch of the vibrational spectrum.

Second, the Macfarlane-Roberts expression is based on a theoretical development[1] which, strictly speaking, applies only to ordered crystals. In order to justify the application of this expression to disordered crystals (Ge-Si alloys), allowance must be made for the fact that the electronic and phonon wave functions for disordered crystals do not have forms as simple as their counterparts in ordered crystals. As will be explained more fully later, Eq. (1) can indeed be applied to disordered crystals, provided the electronic wave functions bear a substantial resemblance to those in ordered crystals.

Returning to the first point, we observe that Eq. (1) is actually a simplified version of the more general six-phonon expression

$$K(h\nu,T)=\sum_{i=1}^{6} A_i\left[\frac{(h\nu-E_g-k\theta_i)^2}{1-\exp(-\theta_i/T)}+\frac{(h\nu-E_g+k\theta_i)^2}{\exp(\theta_i/T)-1}\right], \quad (2)$$

where the summation is carried over the six branches of the vibrational spectrum. In the case of pure Ge, it is possible to show by symmetry arguments[8,23] that the LA (longitudinal acoustical) and TA (transverse acoustical) phonons play a much more important role in the absorption than do the LO (longitudinal optical) and TO (transverse optical) phonons. In the case of Si, similar arguments simply show that all types of phonons can participate in the absorption process. There is a distinction between Ge and Si because the conduction band minima in the former lie at symmetry *points* (the centers of the hexagonal faces of the reduced zone), while those in the latter lie along symmetry *axes* (the [100] axes).

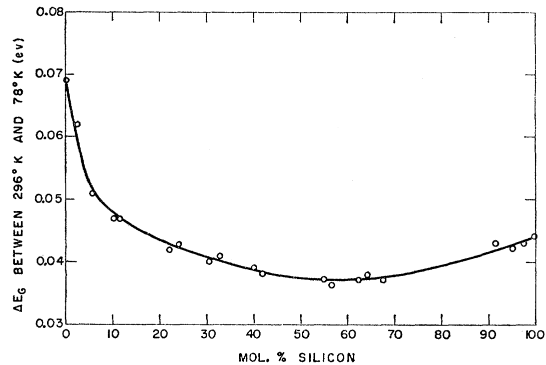

FIG. 15. Composition dependence of change of energy gap between 296°K and 78°K for Ge-Si alloys.

TABLE I. Phonon equivalent temperatures.

	Macfarlane *et al.*[a,b] θ_{LA}	Macfarlane *et al.*[a,b] θ_{TA}	Macfarlane and Roberts θ	Present work θ
Germanium	320°K	90°K	260°K	270±20°K
Silicon	680°K	230°K	600°K	550±50°K

[a] See reference 5.
[b] See reference 6.

[23] F. Herman (unpublished).

Unfortunately, this is about as far as the theory of Ge and Si allows us to go in determining the relative importance of the four terms in Eq. (2). It would be necessary to have a good set of electronic wave functions, a good set of phonon wave functions, and an accurate picture of the electron-phonon interaction to make further progress. At the present time, the only practical approach is to fit Eq. (2) to the experimental absorption spectrum, and thereby determine the relative importance of the various terms empirically.

By making use of high-resolution techniques, Macfarlane *et al.*[5,6] have recently obtained extremely precise absorption spectra for pure Ge and Si. It was found that these spectra could be fitted quite satisfactorily to two-phonon expressions. In each case, the two phonons were identified as the LA and the TA phonons. The results of Macfarlane *et al.* are compared with the earlier one-phonon results of Macfarlane and Roberts[2,3] and with our own phonon results in Table I.

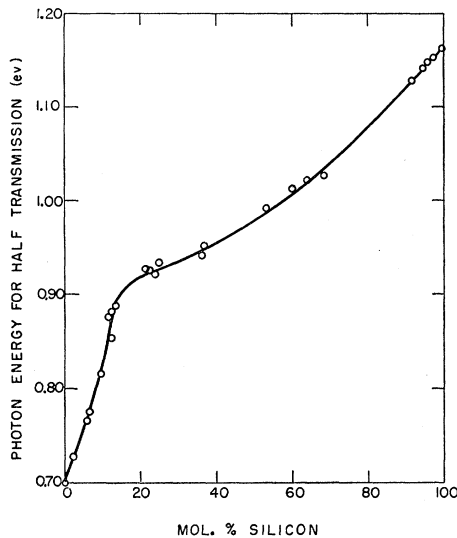

FIG. 16. Composition dependence of photon energy at half transmission in Ge-Si alloys at 296°K. The data have been normalized to a sample thickness of 0.020 in.

It may be seen from Table I that the one-phonon results are essentially weighted averages of the LA and the TA results, with the LA results weighted more heavily than the TA results. We can think of no reason why the weighting factor should be seriously different in the intermediate alloys. Hence, the θ *vs* composition curve shown in Fig. 12 may be regarded as a plot of the average θ *vs* composition; the average θ is expected to approximate, but to be somewhat less than, the equivalent temperature of the LA phonons.

Before discussing the indirect electronic transitions in Ge-Si alloys, it is necessary to make some remarks about the nature of the one-electron states in disordered crystals.

It is well known that each one-electron state in an ordered crystal can be specified by a band index (β) and a reduced wave vector ($\mathbf{k}$). For the purposes of this discussion, it will be assumed that electronic states in disordered crystals can be similarly specified. A theoretical justification for this point of view may be found in a series of papers by Parmenter.[24]

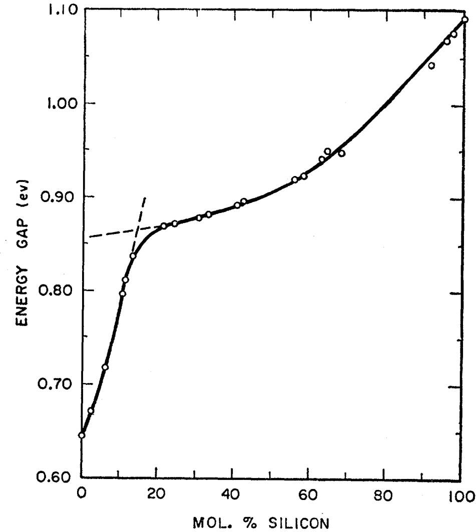

FIG. 17. Composition dependence of energy gap in Ge-Si alloys at 296°K, based on one-phonon Macfarlane-Roberts expression; see Eq. (1) in text.

Since all the Bloch functions $\psi_\beta(\mathbf{k},\mathbf{r})$ for an ordered crystal form a complete set of functions, the wave function $\phi_{\beta'}(\mathbf{k}',\mathbf{r})$ for any state β', $\mathbf{k}'$ in a related disordered crystal may be expanded in terms of the $\psi_\beta(\mathbf{k},\mathbf{r})$:

$$\phi_{\beta'}(\mathbf{k}',\mathbf{r})=\sum_\beta \sum_{\mathbf{k}} B_{\beta'\beta}(\mathbf{k}',\mathbf{k})\psi_\beta(\mathbf{k},\mathbf{r}). \qquad (3)$$

From a physical standpoint, the mixing of the Bloch functions expressed by Eq. (3) arises from the fact that a given wave function must have the proper nodal structure in each ion-core region. For example, a state at the top of the valence band must have a Ge $4p$ nodal structure within each Ge ion-core region, and a Si $3p$ nodal structure within each Si ion core. This can be realized by a proper choice of the distribution function $B_{\beta'\beta}(\mathbf{k}',\mathbf{k})$. Of course, this function will have a different form depending on whether the expansion is performed in terms of Ge or Si Bloch functions. However, this is immaterial to our argument. The important point is that an electronic wave function in a disordered crystal can be characterized by a distribution function $B_{\beta'\beta}(\mathbf{k}',\mathbf{k})$.

Since the disorder in a germanium-silicon alloy is associated with the replacement of atoms of a given valency by other atoms of the same valency, it is unlikely that the disorder will give rise to localized electronic states. It is more likely that the energy level

[24] R. H. Parmenter, Phys. Rev. **97**, 587 (1955); **99**, 1759 (1956); **104**, 22 (1956); see also reference 9.

distribution will be similar to that in an ordered crystal, except that the density of states may fall to zero gradually rather than abruptly, at the limits of each energy band.[24] In other words, the wave functions given by Eq. (3) are expected to describe nonlocalized (band) states rather than localized (impurity) states.

In pure Ge and Si optical absorption at the threshold cannot be produced by the excitation of electrons from the top of the valence band to the bottom of the conduction band since the crystal momentum would not be conserved in such a process. In the case of Ge-Si alloys this process can take place, in principle, provided the disorder produces a substantial mixing of the various Bloch states. This may be seen by examining the optical matrix element

$$P_{\beta'\beta''}(\mathbf{k}',\mathbf{k}'')=-i\hbar\int \phi_{\beta''}^*(\mathbf{k}'',\mathbf{r})\mathbf{e}_q\cdot\nabla\phi_{\beta'}(\mathbf{k}',\mathbf{r})d\mathbf{r}, \quad (4)$$

where the initial and final states are denoted by β', $\mathbf{k}'$ and β'', $\mathbf{k}''$, respectively, and where $\mathbf{e}_q$ is the polarization vector of the incident photon. Substituting the alloy wave functions (3) into (4), we obtain

$$\begin{aligned}P_{\beta'\beta''}(\mathbf{k}',\mathbf{k}'')&=-i\hbar\sum_{\beta_1}\sum_{\mathbf{k}_1}\sum_{\beta_2}\sum_{\mathbf{k}_2}B_{\beta''\beta_2}^*(\mathbf{k}'',\mathbf{k}_2)\\&\quad\times B_{\beta'\beta_1}(\mathbf{k}',\mathbf{k}_1)\\&\quad\times\int\psi_{\beta_2}^*(\mathbf{k}_2,\mathbf{r})\mathbf{e}_q\cdot\nabla\psi_{\beta_1}(\mathbf{k}_1,\mathbf{r})d\mathbf{r} \quad (5)\\&=-i\hbar\sum_{\beta_1}\sum_{\beta_2}\sum_{\mathbf{k}}B_{\beta''\beta_2}^*(\mathbf{k}'',\mathbf{k})B_{\beta'\beta_1}(\mathbf{k}',\mathbf{k})\\&\quad\times\int\psi_{\beta_2}^*(\mathbf{k},\mathbf{r})\mathbf{e}_q\cdot\nabla\psi_{\beta_1}(\mathbf{k},\mathbf{r})d\mathbf{r}.\end{aligned}$$

The reduction from the first to the second form follows from the vertical selection rule for Bloch functions; i.e., the integrals vanish unless $\mathbf{k}_1=\mathbf{k}_2=\mathbf{k}$. The magnitude of the optical matrix element, and hence the strength of the optical absorption, is determined by the degree of overlapping of the distribution functions for the initial and final states in $\mathbf{k}$ space.

If the overlapping were considerable, we would expect to find an essentially temperature-independent component in the absorption spectrum near the threshold. This component would be truly temperature-independent if the band structure did not change with temperature. Since the band structure actually does change slightly with temperature, the disorder-induced absorption near the threshold would exhibit a slight dependence on temperature. However, this can be readily distinguished from the much stronger temperature dependence characteristic of phonon-induced absorption, which is due to the marked change in the phonon population with temperature.

We have found that the experimental absorption curves can be fitted quite successfully to the strongly temperature-dependent expression given by (1). Moreover, after this fit has been made, there is no weakly temperature-dependent residue which could be ascribed to disorder-induced absorption. Therefore, we conclude that the dominant absorption mechanism near the threshold is phonon-assisted indirect electronic transitions. While our work does not rule out the possibility of disorder-assisted indirect electronic transitions, it does indicate that this mechanism is at best of minor importance.

It may be implied from this result that the distribution functions for the initial and final states do not overlap appreciably in the reduced zone. It is likely that these functions are sharply peaked at the different positions in the reduced zone corresponding to the valence and conduction band edges. The prescribed nodal structure of the alloy wave functions is probably achieved by a combination of strong interband mixing and strong local intraband mixing. In the case of the conduction band wave functions, there is probably an additional intervalley mixing. In any event, the distribution functions for the states at the conduction band edge would be quite small in the neighborhood of the valence band edge, and vice versa.

The essential idea here is that the alloy wave functions at the valence and conduction band edges are constructed from sets of Bloch functions having reduced wave vectors belonging to different portions of the reduced zone. If each Bloch function appearing in (3) were expanded in plane waves, we would obtain a Fourier spectrum for each alloy wave function which would be sharply peaked at certain positions in reciprocal space. The normal modes of vibration can also be represented by Fourier series. There will always be some group of phonons whose Fourier spectrum is such as to permit conservation of crystal momentum in a phonon-assisted indirect electronic transition.

These remarks suggest that the theory of phonon-assisted indirect electronic transitions for disordered crystals (in particular, Ge-Si alloys) should bear a close formal resemblance to that for ordered crystals (pure Ge and Si). Accordingly, we may apply the Macfarlane-Roberts expression [see Eq. (1) above] to the alloys with some degree of confidence.

We shall next attempt to interpret the θ *vs* composition curve shown in Fig. 12, which was obtained by fitting the Macfarlane-Roberts expression to the experimental absorption spectra for a number of alloy samples. The S-like trend of the results suggests that the average phonon energy is relatively insensitive to composition at both ends of the composition range. If we were able to calculate the normal modes of vibration for disordered crystals and their composition dependence, we might be able to account for this behavior. Since we are not able to do this, owing to the mathematical complications arising from the disorder, we shall approximate the Ge-Si alloys by two simple models and calculate some normal modes for these models.

While the disorder is ignored in each of these two models, allowance is made for a change of composition. By working with ordered crystals rather than with disordered crystals, the normal modes can be calculated with relative ease.

For future reference, we note that the lattice vibrational Hamiltonian for a Ge-Si alloy has the form

$$\mathcal{H}=-\tfrac{1}{2}\hbar^2[\sum_{\mathrm{Ge}} M_{\mathrm{Ge}}^{-1}\partial^2/\partial X_{\mathrm{Ge}}^2+\sum_{\mathrm{Si}} M_{\mathrm{Si}}^{-1}\partial^2/\partial X_{\mathrm{Si}}^2] +\tfrac{1}{2}[\sum_{\mathrm{Ge}}\sum_{\mathrm{Ge}} X_{\mathrm{Ge}}X_{\mathrm{Ge}}\partial^2\phi/\partial X_{\mathrm{Ge}}\partial X_{\mathrm{Ge}} +\sum_{\mathrm{Ge}}\sum_{\mathrm{Si}} X_{\mathrm{Ge}}X_{\mathrm{Si}}\partial^2\phi/\partial X_{\mathrm{Ge}}\partial X_{\mathrm{Si}} +\sum_{\mathrm{Si}}\sum_{\mathrm{Si}} X_{\mathrm{Si}}X_{\mathrm{Si}}\partial^2\phi/\partial X_{\mathrm{Si}}\partial X_{\mathrm{Si}}], \quad (6)$$

where M_{Ge} and M_{Si} are the masses of Ge and Si atoms, X the nuclear displacement from equilibrium, and ϕ the vibrational potential energy. The summations are carried out over all lattice sites as indicated.

Our first model is based on the so-called virtual-crystal approximation.[25] According to this, a disordered crystal is replaced by an equivalent ordered crystal, in which each lattice site is occupied by the same type of hypothetical atom. This atom is known as a virtual atom. As will be seen below, its properties, e.g., its mass, are uniquely defined by the composition of the virtual crystal.

In this approximation, if the Hamiltonian (6) is averaged over all random configurations consistent with the composition $\mathrm{Ge}_f\mathrm{Si}_{1-f}$, it reduces to

$$\mathcal{H}=-\tfrac{1}{2}\hbar^2 M_f^{-1}\sum_i \partial^2/\partial X_i^2 +\tfrac{1}{2}\sum_i\sum_j X_iX_j[\partial^2\phi/\partial X_i\partial X_j]_f, \quad (7)$$

where the summations on i and j are carried over all lattice sites of the virtual crystal, and where M_f^{-1} and $[\partial^2\phi/\partial X_i\partial X_j]_f$ are defined by

$$M_f^{-1}=fM_{\mathrm{Ge}}^{-1}+(1-f)M_{\mathrm{Si}}^{-1}, \quad (8)$$

$$[\partial^2\phi/\partial X_i\partial X_j]_f =f^2\partial^2\phi/\partial X_{\mathrm{Ge}}\partial X_{\mathrm{Ge}}+2f(1-f)\partial^2\phi/\partial X_{\mathrm{Ge}}\partial X_{\mathrm{Si}} +(1-f)^2\partial^2\phi/\partial X_{\mathrm{Si}}\partial X_{\mathrm{Si}}. \quad (9)$$

According to the virtual-crystal model, an atom with suitably averaged mass, M_f, is placed at each lattice site, and the coupling between any pair of such atoms is described by the averaged coupling factor given by (9). In (9), the right-hand side contains the coupling factors between Ge-Ge, Ge-Si, and Si-Si pairs in the original alloy. If the Ge-Si coupling factor is assumed to be the arithmetic average of the Ge-Ge and the Si-Si coupling factors, (9) reduces to:

$$[\partial^2\phi/\partial X_i\partial X_j]_f=f\partial^2\phi/\partial X_{\mathrm{Ge}}\partial X_{\mathrm{Ge}} +(1-f)\partial^2\phi/\partial X_{\mathrm{Si}}\partial X_{\mathrm{Si}}. \quad (10)$$

[25] L. Nordheim, Ann. Physik **9**, 607, 641 (1931); T. Muto, Sci. Papers Inst. Phys. Chem. Research (Tokyo) **34**, 377 (1938); see also references 9 and 22.

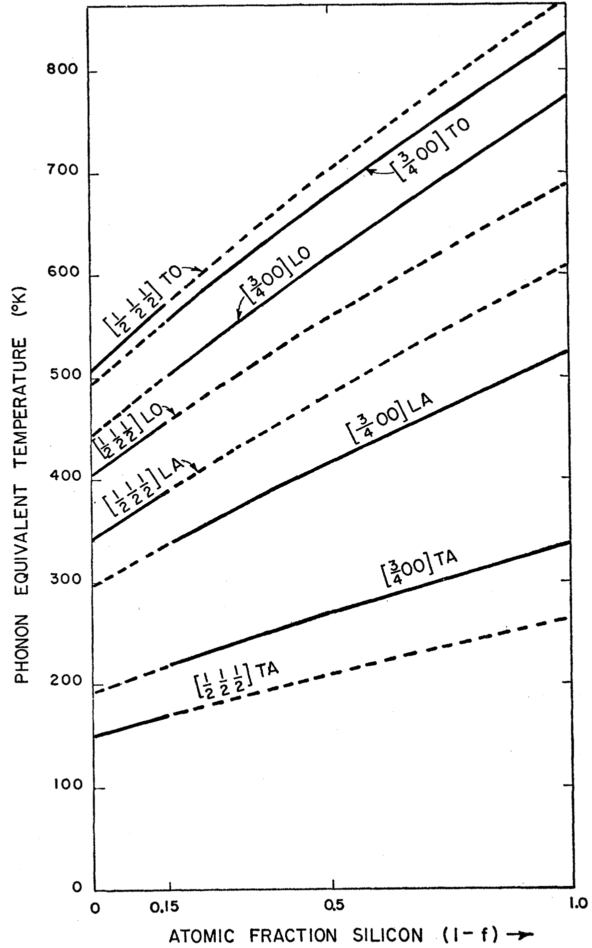

FIG. 18. Variation of phonon energy (expressed as equivalent temperature) with composition according to virtual-crystal approximation. The results shown are for the four [111] phonons at $\mathbf{k}=(2\pi/a)[\frac{1}{2},\frac{1}{2},\frac{1}{2}]$, and for the four [100] phonons at $\mathbf{k}=(2\pi/a)\times[\frac{3}{4},0,0]$. Since the exact position of the conduction band edge in pure Si is not known, we have arbitrarily placed it at $\mathbf{k}=(2\pi/a)\times[\frac{3}{4},0,0]$. It has been assumed that the conduction band edge remains at $\mathbf{k}=(2\pi/a)[\frac{1}{2},\frac{1}{2},\frac{1}{2}]$ in the range 0 to 15 atomic percent Si, and at $\mathbf{k}=(2\pi/a)[\frac{3}{4},0,0]$ in the remaining composition range.

This approximation completely neglects the fact that the coupling between any pair of atoms in the original alloy may depend upon their local environments. Thus, the coupling terms on the right-hand side of (9) and (10) are themselves average quantities.

Using the force model described in the Appendix, we have calculated the normal mode frequency as a function of composition for a number of normal modes. In this work, $\partial^2\phi/\partial X_{\mathrm{Ge}}\partial X_{\mathrm{Ge}}$ and $\partial^2\phi/\partial X_{\mathrm{Si}}\partial X_{\mathrm{Si}}$ were represented by their counterparts in pure Ge and Si crystals. The results of the calculation are shown in Fig. 18. It may be seen that the virtual-crystal model predicts an essentially linear variation with composition for each normal mode. According to this model, θ should vary linearly with composition in the 0–15% Si range ([111] phonons) and in the 15–100% Si range ([100]

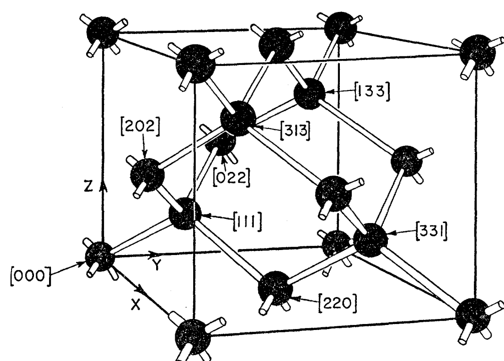

FIG. 19. The eight atomic positions in the unit cube of a diamond-type lattice. The Cartesian coordinates are given in units of $a/4$, where a is the unit cube edge.

phonons); at 15% Si, there should be a slight discontinuity in θ, due to the change-over from [111] to [100] phonons. Clearly, these predictions are not substantiated by the experimental result (see Fig. 12), which gives an S-like curve with no apparent discontinuity at 15% Si.

It is hardly surprising that our analysis of the experimental data, which leads to Fig. 12, fails to show up a discontinuity in θ at 15% Si. Since the [111] and the [100] LA phonons have nearly the same energies at this composition, the discontinuity is small, and hard to detect. Furthermore, in the neighborhood of this composition, indirect electronic transitions take place both to the [100] and the [111] conduction band minima. For this reason the analysis would tend to make θ continuous, rather than discontinuous at the critical composition.

In the case of long-wavelength acoustical modes, the virtual-crystal approximation should be quite satisfactory, since the specific arrangement of the atoms among the available lattice sites is essentially irrelevant. The frequencies of such modes should depend on the average force constants between various pairs of atoms, and on the average mass of these atoms. These are just the quantities on which the virtual-crystal model is based.

In the case of short-wavelength modes, which are of particular interest here, the virtual-crystal approximation fails badly, as is indicated by the discrepancy between Figs. 12 and 18. It must be concluded, therefore, that the composition dependence of the short-wavelength mode frequencies is determined by some feature of the physical problem neglected in this approximation.

The most obvious shortcoming of the virtual-crystal model is the placement of only one type of atom (the virtual atom) at each lattice site. In the model to be considered below, the Ge-Si alloy system will be simulated by a series of ordered crystals formed from Ge and Si atoms arranged in different ways among the sites of a diamond-type lattice. This model is more realistic than the virtual-crystal model for two reasons. In the first place, it makes allowance for the fact that there are two types of atoms present, rather than just one type. Secondly, it introduces short-range order into the problem. Although there is no experimental evidence that any substantial degree of short-range order is actually present in the Ge-Si alloy system, it is not unreasonable to expect some short-range order. In this case, the atoms of one type will tend to avoid being nearest neighbors of each other. This tendency is accentuated by the ordered-crystal model.

Since a diamond-type lattice is composed of eight interpenetrating simple cubic lattices, (see Fig. 19) it is convenient to work with a series of ordered crystals having the compositions Ge_fSi_{1-f}, where $f=0$, 1/8, 2/8 $\cdots$ 8/8. This series, which contains 15 physically distinct members, can be generated by placing Ge or Si atoms at the sites of each of the eight cubic sublattices, and varying the composition and the atomic structure. Each member in the series can be characterized by a particular arrangement of the $8f$ Ge atoms and the $8(1-f)$ Si atoms among the eight positions in the unit cell, which may be taken as the unit cube of the diamond-type lattice. The 15 physically distinct arrangements are listed in Table II. All others yield ordered crystals physically indistinguishable from those already given in this table.

Because the direct lattice of the generic ordered crystal (GOC) is a simple cubic lattice, the reciprocal lattice is also a simple cubic lattice, and the reduced zone is a cube. In Fig. 20 the first and second zone in the plane $k_z=0$ for GOC are indicated by the dotted lines, and the first (reduced) zone for the diamond-type lattice is indicated by the full lines. It can be seen from this figure that the central point of the reduced zone for the GOC corresponds to $\mathbf{k}=(2\pi/a)[000]$, $(2\pi/a)\times[100]$, $(2\pi/a)[010]$, and $(2\pi/a)[001]$ for the diamond-type lattice. Since the GOC is a three-dimensional

TABLE II. Ordered crystals: arrangement of Ge and Si atoms in unit cell.

Case	Atomic fraction Si: $(1-f)$	Position in unit cell [in units of $a/4$, where a is lattice constant (unit cube edge)] [000]	[111]	[022]	[133]	[202]	[313]	[220]	[331]
0	0	Ge	Ge	Ge	Ge	Ge	Ge	Ge	Ge
1	1/8	Si	Ge	Ge	Ge	Ge	Ge	Ge	Ge
2	2/8	Si	Ge	Si	Ge	Ge	Ge	Ge	Ge
3	3/8	Si	Ge	Si	Ge	Si	Ge	Ge	Ge
4	4/8	Si	Ge	Si	Ge	Si	Ge	Si	Ge
5	5/8	Si	Si	Si	Ge	Si	Ge	Si	Ge
6	6/8	Si	Si	Si	Si	Si	Ge	Si	Ge
7	7/8	Si	Si	Si	Si	Si	Si	Si	Ge
8	1	Si	Si	Si	Si	Si	Si	Si	Si
2′	2/8	Si	Si	Ge	Ge	Ge	Ge	Ge	Ge
3′	3/8	Si	Si	Si	Ge	Ge	Ge	Ge	Ge
4′	4/8	Si	Si	Si	Si	Ge	Ge	Ge	Ge
5′	5/8	Si	Si	Si	Si	Si	Ge	Ge	Ge
6′	6/8	Si	Si	Si	Si	Si	Si	Ge	Ge
4″	4/8	Si	Si	Si	Ge	Si	Ge	Ge	Ge

structure having eight atoms per unit cell, there are 24 normal modes associated with each point in its reduced zone. In the special case of the central zone point, the 24 modes have the same translational periodicity as the 24 modes in diamond-type crystals having the four reduced wave vectors mentioned above. Six of these modes correspond to $\mathbf{k}=(2\pi/a)[000]$, and the remaining eighteen to $\mathbf{k}=(2\pi/a)[100]$, $(2\pi/a)[010]$, and $(2\pi/a)[001]$. By following the behavior of these eighteen as a function of composition, it is possible to obtain information about the composition dependence of a certain group of short-wavelength modes in a system which simulates the Ge-Si alloy system.

Using a force model involving nearest-neighbor interactions only, we have calculated the 24 normal modes for each of the 15 members of our series. (The details of this calculation will be published elsehwere.)[26] To illustrate the general nature of the result, we have shown all the normal-mode frequencies in Figs. 21 and 22. At each end of the composition range (pure Ge and Si), there are two sets of threefold degenerate modes, and three sets of sixfold degenerate modes. The former correspond to the acoustical (zero frequency) and the optical (Raman frequency) $\mathbf{k}=(2\pi/a)[000]$ modes; the latter correspond to the TA, the coincident LA and LO, and the TO modes for $\mathbf{k}=(2\pi/a)[100]$, $(2\pi/a)\times[010]$, and $(2\pi/a)[001]$ modes. As we proceed across the composition range from either end, the threefold and sixfold degeneracies are removed in a manner consistent with the symmetry of the various crystals in the series.

In presenting these results the 15 crystals in the series were divided into two subseries because the members of each subseries have certain features in common. In the subseries shown in Fig. 21 (let us call this A), one of the face-centered cubic sublattices of the diamond-type lattice is progressively filled, and then the other, as the composition is changed. This may be clearly seen from Table II and Fig. 19. In this subseries,

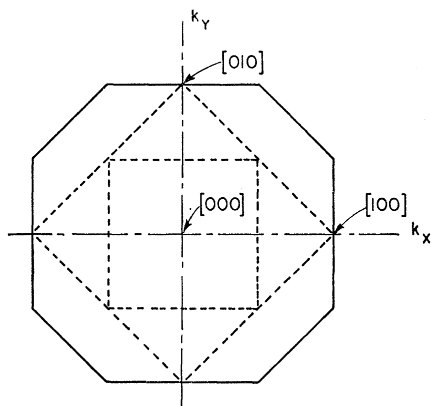

FIG. 20. Zone schemes for diamond-type crystal (full lines) and generic ordered crystal (dotted lines) in the plane $k_z=0$.

[26] F. Herman and S. Skillman (to be published).

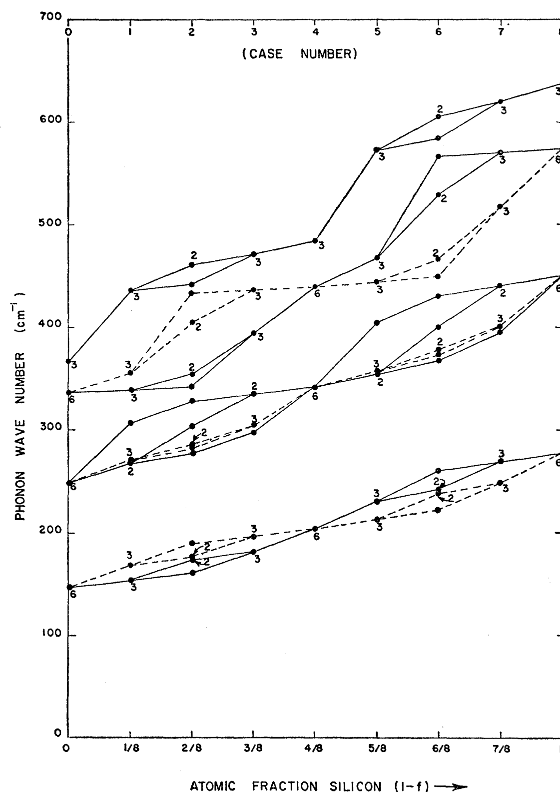

FIG. 21. Variation of phonon energy (expressed as wave number) with composition according to ordered-crystal approximation. The degeneracy of each normal mode (if other than unity) is indicated. Normal modes having similar vibrational patterns are shown connected. The results shown are for cases 0, 1, 2, 3, 4, 5, 6, 7, and 8.

the minority atoms occur only as next-nearest neighbors (cases 2, 3, 5, 6); in the middle of the composition range, the atoms of one type (Ge or Si) also occur only as next-nearest neighbors (case 4). In the subseries shown in Fig. 22 (let us call this B), the minority atoms occur as nearest and next-nearest neighbors (cases 2′, 3′, 5′, and 6′); the same is true for the atoms of each type in the middle of the range (cases 4′ and 4″). Of course, the cases 0, 1, 7, and 8 are common to both subseries.

From the above characterization, it may be seen that there is more "short-range order" in subseries A than in subseries B; i.e., the atoms of each type avoid each other more fully in the former than in the latter.

To illustrate the spread in the normal modes associated with each set of normal modes in pure Ge and Si, we have drawn the envelopes of these modes in Fig. 23. For clarity, we have drawn a vertical line through the various modes derived from a particular set of modes in pure Ge and Si at each intermediate composition. For the purposes of comparison, we have calculated the corresponding sets of normal modes on the basis of the virtual-crystal approximation and the same force system (see the Appendix). These are shown in Fig. 23 by the broken lines. It may be seen that there

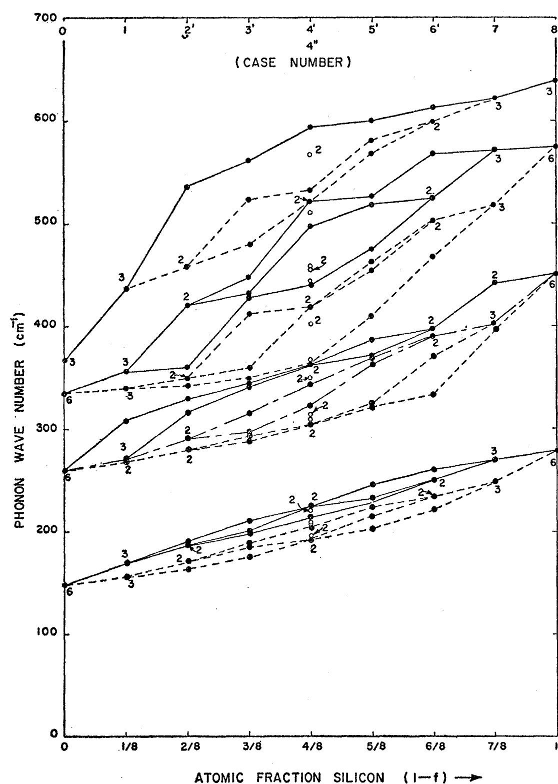

FIG. 22. Variation of phonon energy (expressed as wave number) with composition according to ordered-crystal approximation. The degeneracy of each normal mode (if other than unity) is indicated. Normal modes having similar vibrational patterns are shown connected. The results for cases 0, 1, 2′, 3′, 4′, 5′, 6′, 7, and 8 are given by heavy dots; those for case 4″ are given by open circles.

is a considerable spread in the frequencies of the normal modes belonging to each group. This spread increases as we move toward the middle of the composition range from either end.

Figure 23 shows that the short-wavelength normal modes in crystals containing two types of atoms can depart quite markedly from their counterparts in geometrically similar crystals containing only one type of atom. Undoubtedly, part of the spread can be attributed to the use of ordered crystals. However, by comparing the results in Figs. 21 and 22 for different pairs of ordered crystals having the same compositions, e.g., cases 2 and 2′, it may be seen that some of the spread in the normal modes in each group is common to both members of the pair. Since there is a common spread in different ordered crystals having the same composition, it is reasonable to conclude that this part of the spread, at least, is due to the presence of two types of atoms. It may be further concluded that even in disordered crystals containing two types of atoms, there will be a spread in the normal modes derived from a particular set of normal modes in a related ordered crystal.

The ordered-crystal model has introduced the crucial factor of atoms with two distinct masses in a systematic, albeit oversimplified fashion. We may therefore expect that the calculated distribution of short-wavelength modes and the variation of this distribution with composition (as exemplified by Figs. 21 and 22) will be closer to the actual case of the Ge-Si alloys than similar calculations based on an averaged or virtual-crystal model.

Let us now go one step further. By examining the eigenvectors associated with each mode,[26] it is possible to determine the vibrational patterns of the various modes. The modes can then be arranged into groups, such that for each group the vibrational pattern changes in a more or less progressive fashion as the composition is changed. Since we are interested primarily in the behavior of the short-wavelength modes, we shall confine ourselves in the discussion to follow to groups of modes which terminate at the six-fold degenerate modes at each end of the composition range.

In the case of series A (see Fig. 21), the lines connecting the normal modes in nearly each group form S-shaped and inverted S-shaped curves; in the case of series B (see Fig. 22), these lines form convex and concave curves. These four curves are shown schematically in Fig. 24.

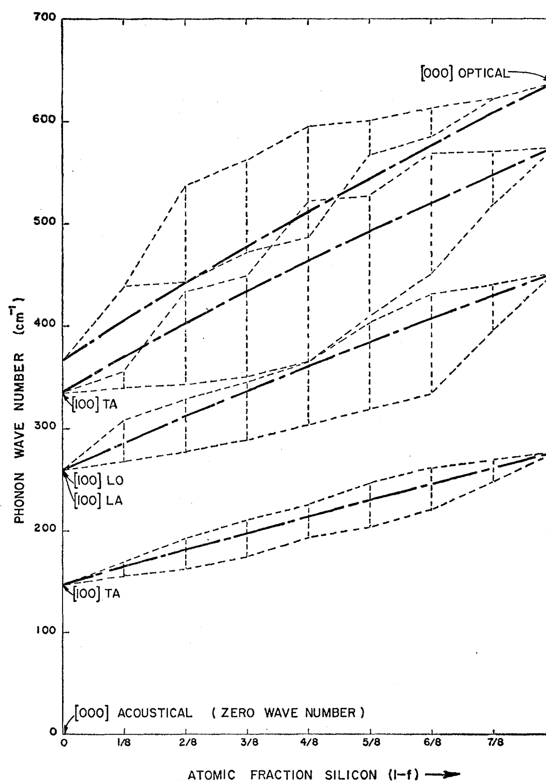

FIG. 23. Comparison of normal modes in virtual crystals (broken lines) with associated normal modes in ordered crystals (dotted lines). Each vertical dotted line indicates the maximum spread of the normal modes derived from a particular set of normal modes in pure Ge and Si.

Using Fig. 24 as a guide, we may now turn to the actual Ge-Si alloy system, to which the ordered-crystal system is admittedly a very crude approximation, and predict that the short-wavelength normal modes vary with composition in any one of the four ways indicated by this figure. It is tempting to assume that the phonons most effective in inducing indirect electronic transitions are those described by the S-shaped curve in Fig. 24(a), since this has the same form as the data in Fig. 12. However, we have no theoretical basis for making this assumption. About the most we can say is that the ordered-crystal model predicts four types of behavior, one of which closely resembles the experimental result.

In effect, Fig. 12 suggests that of all the normal modes in the Ge-Si alloy system, there are some which are best able to satisfy the crystal momentum conservation condition required for indirect electronic transitions. This means that the Fourier distributions of these normal modes are strongly peaked at the appropriate positions in reciprocal space. Why this should be so for the normal modes which follow an S-shaped curve, rather than any of the three other curves in Fig. 24, is somewhat of a mystery. However, it is worth noting that the S-shaped curve is associated with the subseries which has the greater degree of short-range order. It would indeed be interesting if some independent experimental evidence could be obtained for the presence of short-range order in the Ge-Si alloy system.

ACKNOWLEDGMENTS

The authors wish to express their appreciation to a number of their colleagues at the RCA Laboratories for their assistance and cooperation in the various phases of this work. In particular, the authors are grateful to Dr. H. Johnson, Dr. L. S. Nergaard, and Dr. D. O. North for their constant encouragement; to Dr. S. M. Christian for providing the many samples used in this investigation; to Dr. M. C. Gardels for determining the composition of these samples; to Mr. J. J. Gannon for able assistance in performing some of the measurements; and to Mr. S. Skillman for programming the necessary calculations on an IBM 650 Magnetic Drum Calculator.

Finally, the authors wish to thank Dr. J. O. Kessler, Mr. M. A. Lampert, Dr. R. H. Parmenter, and Dr. P. J. Wojtowicz for their critical comments on the manuscript.

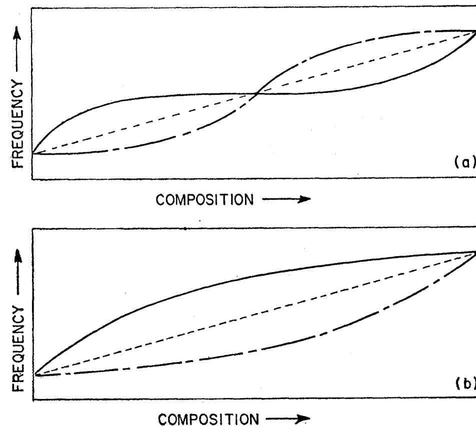

FIG. 24. Schematic diagram of variation of normal mode frequencies with composition in ordered crystal system; (a) refers to the subseries shown in Fig. 21, and (b) to the subseries shown in Fig. 22. The dotted lines suggest the linear behavior characteristic of the virtual-crystal model.

APPENDIX

The calculations leading to the normal-mode frequencies of the virtual crystals (see Fig. 18) were based on a three-parameter force model involving general forces between nearest neighbors, and angular forces between next-nearest neighbors. Nearly all the information required to carry out these calculations is contained in the paper by Smith.[27] The general forces between nearest neighbors are described by Smith's parameters α and β. Before commenting on the angular forces, it should be pointed out that there is an error in Smith's treatment of the next-nearest neighbor dynamical matrices. In the case of a force model involving general next-nearest neighbor forces, Smith's work suggests that there are only three independent dynamical matrix elements, μ, ν, and λ. Actually, there is a fourth, call it δ, which Smith incorrectly set equal to zero. Thus, the correct form of D^9 [see Smith's Eq. (2.32)] is[23]

$$-(1/M)\begin{vmatrix} \mu & \nu & \delta \\ \nu & \mu & \delta \\ -\delta & -\delta & \lambda \end{vmatrix}$$

rather than

$$-(1/M)\begin{vmatrix} \mu & \nu & 0 \\ \nu & \mu & 0 \\ 0 & 0 & \lambda \end{vmatrix}.$$

If it is assumed, as we have done, that the next-nearest neighbor dynamical matrices describe angular forces, rather than general forces, it is easily shown that

$$\mu=\nu=\delta/2=-\lambda/4.$$

Thus, our force model involves three independent parameters, α, β, and μ.

The values of these three parameters can be determined by fitting the theory to the experimental values for the three elastic constants[28] (c_{11}, c_{12}, and c_{44}). The experimental information, including that for the lattice constants,[29] and the derived results for α, β, and μ are given in Table III. In this table, M^{-1} represents the reciprocal atomic mass.

In the interest of simplicity, the next-nearest neighbor parameters were set equal to zero in the calculations

[27] H. M. J. Smith, Trans. Roy. Soc. (London) **A241**, 105 (1948); see also Y.-C. Hsieh, J. Chem. Phys. **22**, 306 (1954).
[28] H. J. McSkimin, J. Appl. Phys. **24**, 988 (1953).
[29] A. Smakula and J. Kalnajs, Phys. Rev. **99**, 1737 (1955).

TABLE III. Experimental data and derived parameters.

	a (10^{-8} cm)	ac_{11}	ac_{12}	ac_{44} (10^4 dyne/cm)	α	β	μ	M^{-1} (10^{22} g^{-1})
Si	5.4307	8.991	3.467	4.317	8.423	5.235	0.071_0	2.1446
Ge	5.6575	7.295	2.735	3.799	7.221	4.869	0.010_4	0.8293_7

leading to Figs. 21, 22, and 23, while the same values of α and β were used as before. Since μ is much smaller than α or β (according to our model), this influences the results only slightly.

By comparing the experimental results of Macfarlane *et al.*[5,6] for θ_{LA} and θ_{TA} for pure silicon and germanium [see Table I] with those given by our calculations [see Fig. 18], it may be seen that there is a serious disagreement between these two sets of results. We have attempted to remedy this situation by constructing a number of five-parameter force models involving the two first-neighbor parameters α and β, and three independent second and/or third neighbor parameters. In each case, the five parameters were evaluated by fitting the theory to the experimental values of c_{11}, c_{12}, c_{44}, θ_{LA}, and θ_{TA}. Unfortunately, these models predict Raman frequencies which are unreasonably low. Since we have been unable to find a force system which fits all the available experimental information, and which at the same time appears physically realistic, we are reporting only the results for the original three-parameter force model.

Since the difference in the atomic masses for silicon and germanium accounts almost entirely for the difference in their lattice spectra, the choice of a force model is not as critical a matter as it would be otherwise. Even if we had assumed the same force system for silicon and germanium, the qualitative features of Figs. 18, 21, 22, and 23 would remain essentially the same. However, it is rather disturbing that we were unable to find a satisfactory force model within the framework of the Born-Smith theory.

PHYSICAL REVIEW VOLUME 109, NUMBER 3 FEBRUARY 1, 1958

Electrical Conductivity of X-Irradiated NaCl

R. W. CHRISTY AND W. E. HARTE*
Dartmouth College, Hanover, New Hampshire
(Received September 16, 1957)

The electrical resistance of Harshaw sodium chloride crystals exposed at room temperature to x-ray doses sufficient to produce about 6×10^{16} F centers/cm^3 has been measured as a function of time at constant temperatures between 150 and 200°C. The effects of previous heat treatment of the crystals, x-ray dose, temperature of measurement, and preliminary optical bleaching have been observed. Initially the resistance of irradiated crystals is much greater than that of unirradiated ones. The resistance of the colored crystals at first decreases rapidly (for about 10 to 100 minutes, depending on the temperature). In the case of crystals used as received from Harshaw, the resistance even falls slightly below that of the normal uncolored crystals. Subsequently the resistance again increases, reaching a constant value (after about 50 to 1000 minutes) higher than for the normal crystal. If the crystals are optically bleached before the measurement, the resistance increase recovers very much more slowly. The behavior can be restored to normal by annealing above 250°C. The slow resistance increase is seen as evidence for the production by the x-rays of excess positive-ion vacancies.

I. INTRODUCTION

LARGE increases of electrical resistivity have been observed in sodium chloride and other alkali halide crystals which have been subjected to ionizing radiation, whether gamma rays,[1] x-rays,[2] or protons.[3,4] These radiations also produce color centers in the crystals,[5] so that such changes should be expected if formation of some of the color centers involves neutralization or immobilization of charge carriers. Since these crystals are ionic conductors in which only positive ion vacancies are mobile at low temperatures,[6] the capture of a positive hole formed by the radiation at a positive-ion vacancy in the lattice, i.e., according to Seitz's model[5] the formation of a V_1 center, would be such an event. (The V_1 centers actually are unstable at room temperature, but other more complicated possibilities exist.)

On the other hand, since the number of color centers deduced from the intensity of coloration is greater than the number of vacancies thought to be normally present in the lattice, it is believed that the ionizing radiation is also capable of producing extra vacancies. In fact, density changes accompanying irradiation have

---

* Now at the University of Maryland, College Park, Maryland.
[1] Nelson, Sproull, and Caswell, Phys. Rev. **90**, 364 (1953).
[2] F. A. Cunnell and E. E. Schneider, Phys. Rev. **95**, 598 (1954).
[3] E. A. Pearlstein, Phys. Rev. **92**, 881 (1953).
[4] K. Kobayashi, Phys. Rev. **102**, 348 (1956).
[5] For a review, see F. Seitz [Revs. Modern Phys. **26**, 7 (1954)].
[6] Tubandt, Reinhold, and Leibold, Z. anorg. u. allgem. Chem. **197**, 225 (1931).